COMMUNICATION

Check for updates

Enhanced electrochemiluminescence imaging of single cell membrane proteins based on Co₃O₄ nanozyme catalysis†

Jingjing Zhang,[a] Lin Hao,*[b] Jie Chao,[a] Lianhui Wang [iD][c] and Shao Su [iD]*[c]

The development of enhanced strategies with excellent biocompatibility is critical for electrochemiluminescence (ECL) imaging of single cells. Here, we report an ECL imaging technique for a single cell membrane protein based on a Co₃O₄ nanozyme catalytic enhancement strategy. Due to the remarkable catalytic performance of Co₃O₄ nanozymes, H₂O₂ can be efficiently decomposed into reactive oxygen radicals, and the reaction with L012 was enhanced, resulting in stronger ECL emission. The anti-carcinoembryonic antigen (CEA) was coupled with nanozyme particles to construct a probe that specifically recognized the overexpressed CEA on the MCF-7 cell membrane. According to the locally enhanced visualized luminescence, the rapid ECL imaging of a single cell membrane protein was eventually realized. Accordingly, Co₃O₄ nanozymes with highly efficient activity will provide new insights into ECL imaging analysis of more biological small molecules and proteins.

Electrochemiluminescence (ECL) is a kind of optical radiation phenomenon produced by chemical molecules undergoing electrochemical reaction.[1–3] ECL does not require an additional excitation light source, since the reaction process depends on the applied voltage to drive the luminescence process, which effectively avoids the interference of light scattering and improves the detection sensitivity. It has become a powerful analytical technique, widely used in biochemical analysis,[4] pharmaceutical analysis,[5] environmental analysis[6] and other fields. In view of the urgent need for high analytical throughput and spatial resolution, ECL imaging was created by coupling

a School of Geographic and Biologic Information, Nanjing University of Posts and Telecommunications, Nanjing 210023, China

b Department of Urology, Xuzhou Central Hospital, Xuzhou 221009, Jiangsu, China. E-mail: haolinxuzhou@163.com

c Key Laboratory for Organic Electronics and Information Displays, Jiangsu Key Laboratory for Biosensors, Institute of Advanced Materials (IAM), Jiangsu National Synergetic Innovation Center for Advanced Materials (SICAM), Nanjing University of Posts and Telecommunications, Nanjing 210023, China. E-mail: iamssu@njupt.edu.cn

ECL technology with optical microscopy. This new imaging method can not only achieve high-throughput and visualization of biomolecules,[7] but also be applied to the research of spatiotemporal resolution imaging of single entities such as particles, cells and bacteria.[8–12] It can provide more spatial detail information, such as identification of cellular contents and structures. Small molecules in cells or released from cells, (sub-)cellular structures including cell membranes,[13,14] proteins,[10,15] mitochondria[16] and intracellular hierarchical structures such as the nucleolus, nucleus and endoplasmic reticulum[17] have been visualized by ECL imaging.[18] With the enhancement effects of silica nanochannels on ECL intensity, Su *et al.* have explored the dynamic variation of cell–matrix adhesions during collective migration using the negative imaging mode.[19–21] Despite the significant achievements in ECL imaging, it has the technical limitation of insufficient sensitivity and time resolution due to the weak luminescence signal generated by the luminophore. It is a challenge to further develop a novel biocompatible approach of ECL imaging, and enhance the ECL intensity, thereby improving the sensitivity and temporal resolution.
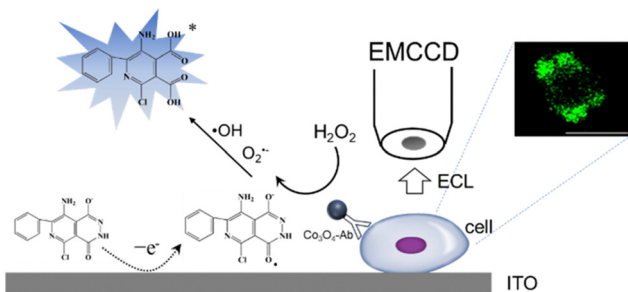
Nanozymes have sparked widespread research due to their unique properties of nanomaterials and catalytic activity.[22–25] They can efficiently catalyze the substrates of enzymes under mild conditions, showing catalytic efficiency and enzymatic reaction kinetics similar to natural enzymes. In view of their advantages such as adjustable catalytic activity, easy large-scale synthesis, higher physiochemical stability, higher durability and lower costs,[26] nanozymes have attracted considerable interest and represent great potential applications in biomedicine, disease diagnosis, the environment and biological detection. Numerous studies have indicated that many nanomaterials have been discovered to possess nanozyme properties, such as Fe₃O₄,[26] AuNPs,[27,28] carbon dots,[29] and so on. Among them, Co₃O₄ nanoparticles, with catalase-like activity, can be adopted as accelerators of H₂O₂ for enhancing the ECL emission of the luminol-H₂O₂ system, because the conversion of the Co²⁺/Co³⁺ redox pair could efficiently excite the generation of electron holes, and then react with the molecular orbital

Scheme 1 ECL mechanism based on the Co_3O_4 nanozyme for CEA antigen imaging at the cellular membrane.

of H_2O_2 for promoting its decomposition.[30] Based on this advantage, the Co_3O_4 nanozyme can be combined with the luminol-H_2O_2 ECL system, and it is expected to significantly improve the ECL intensity, thereby further improving the sensitivity and time resolution of the imaging technology and achieving rapid single-cell ECL imaging analysis.

Herein, a Co_3O_4 nanozyme was used as a catalyst of the luminol-H_2O_2 system for single cell ECL imaging. H_2O_2 produces reactive oxygen species by the catalysis of Co_3O_4. Under the condition of applying a suitable voltage, L012 (a luminol analog with high ECL efficiency) undergoes an electrochemical reaction to produce intermediates, which in turn react with reactive oxygen species to produce an ECL signal (Scheme 1). The ECL intensity of the L012-H_2O_2 system was significantly enhanced and achieved ultra-sensitive visualization of H_2O_2. Subsequently, a Co_3O_4 nanozyme-labeled CEA antibody was used as a probe to achieve sensitive and rapid imaging of CEA at the cellular membrane. This work provides a new approach for high-resolution ECL imaging.

The diameter of the Co_3O_4 nanoparticles used in this study is ~ 30 nm, as characterized in the transmission electron microscopy (TEM) image (Fig. S1, ESI†). To investigate the enhancement effects of the Co_3O_4 nanozyme, the electrochemical and ECL curves of the L012-H_2O_2 system on Co_3O_4 coated ITO electrodes were measured in 10 mM PBS containing 200 μM L012 and 20 μM H_2O_2. From Fig. 1A, in the presence of Co_3O_4, the ECL intensity from L012 and H_2O_2 improved to pprox. 3.0 fold higher than that of the bare ITO electrode. This enhancement should be ascribed to the excellent catalytic
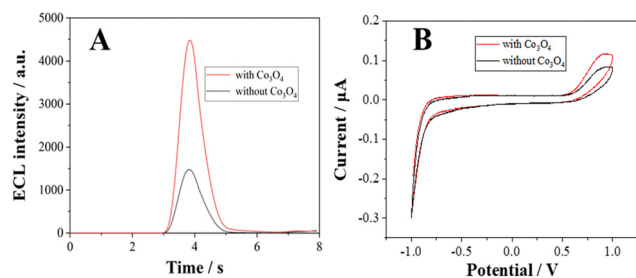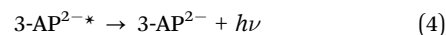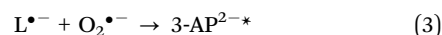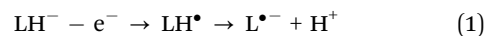
performance of Co_3O_4, which accelerates the decomposition of H_2O_2 to produce reactive oxygen radicals. The corresponding CV curves show that the peak current of the Co_3O_4-coated ITO electrode is significantly enhanced compared with the bare ITO electrode (Fig. 1B), indicating that the presence of Co_3O_4 could promote electron transport. The enhancements of both the ECL and peak current demonstrate that the introduction of Co_3O_4 served as an accelerator promoting the decomposition of coreactant H_2O_2 and enhancing the ECL intensity of the L012-H_2O_2 system. A possible ECL mechanism is proposed (eqn (1)–(4)). L012 anion LH^- is oxidized to radical $L^{\bullet-}$ during the electrochemical scanning. Meanwhile, the Co_3O_4 catalyzes H_2O_2 to produce abundant oxygen radicals $O_2^{\bullet-}$ and $OH^{\bullet}$ on the ITO surface. In addition, Co_3O_4 can facilitate the reaction of $L^{\bullet-}$ and the oxygen radical to generate activated intermediate $3\text{-}AP_2^{-*}$, which goes back to the ground state, generating the ECL emission.

$$LH^- - e^- \rightarrow LH^{\bullet} \rightarrow L^{\bullet-} + H^+ \quad (1)$$

$$H_2O_2 \xrightarrow{Co_3O_4} O_2^{\bullet-} + H^+ \quad (2)$$

$$L^{\bullet-} + O_2^{\bullet-} \rightarrow 3\text{-}AP^{2-*} \quad (3)$$

$$3\text{-}AP^{2-*} \rightarrow 3\text{-}AP^{2-} + h\nu \quad (4)$$

The diluted Co_3O_4 was coated on the ITO slide, which was then placed in 10 mM PBS containing 200 μM L012 and 20 μM H_2O_2, and the ECL signal was generated by applying a conversion mode voltage between 1.0 V (2 s) and −1.0 V (0.5 s) using a voltage transmitter. The ECL images were obtained using EMCCD with an exposure time of 1 s by applying 1.0 V voltage. Fig. S2 (ESI†) shows the bright-field and ECL image of Co_3O_4 on the ITO slide. The light spots generated in the ECL image can coincide with the particles in the bright field image, indicating that the presence of Co_3O_4 produces locally enhanced light spots. In addition, the voltage from 0.5 V to 1.2 V at the ITO slide was applied to induce ECL. The distinguished luminescence spots at Co_3O_4 nanoparticles can be clearly seen under a voltage of 0.7 V from Fig. 2, while no luminescence is recorded from the ITO slide, which is attributed to the fact that Co_3O_4 can catalyze the L012-H_2O_2 system to produce locally enhanced signals. When the applied voltage reaches 1.0 V, the luminescence spots can be seen from all the Co_3O_4 nanoparticles.
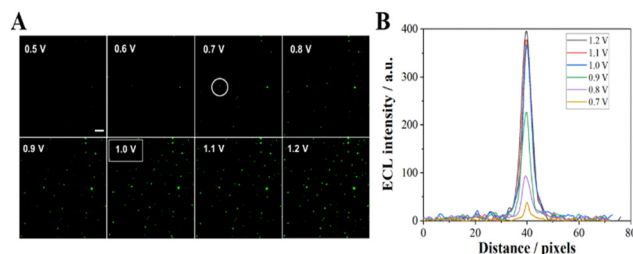

Fig. 1 (A) ECL profiles and (B) CV curves of the L012-H_2O_2 system at the ITO surface with and without Co_3O_4. Working solution: 10 mM PBS containing 200 μM L012. Scan range: −1.0 to 1.0 V, scan rate: 0.1 V s^{-1}, PMT voltage: 600 V.

Fig. 2 (A) ECL image of Co_3O_4 at the ITO slides with different applied potentials; the exposure time was 1 s. (B) The luminescence intensity across the particle circle in image A. Scale bar: 5 μm.

A continuous increase in the voltage from 0.5 to 1.2 V results in an increase in the ECL intensity from the Co_3O_4 particle (Fig. 2B), which is consistent with our previous observation. When the voltage exceeds 1.0 V, the increase in ECL intensity is not significant, therefore 1 V was selected as the ECL imaging voltage.

The effect of exposure time on ECL imaging was also explored. Under the condition of applied voltage at 1 V, when the exposure time is 500 ms, all the particles at the ITO interface produce clearly distinguishable luminescence spots (Fig. 3). Compared with the previous ECL imaging analysis,[12,31,32] the presence of the Co_3O_4 nanozyme can shorten the exposure time obviously, indicating that the catalytic activity of the Co_3O_4 nanozyme can significantly enhance the ECL luminescence of the L012-H_2O_2 system, endowing it with higher temporal resolution. In addition, the stability of ECL luminescence using the Co_3O_4 nanozyme as a catalyst was also investigated. As shown in Fig. 4, the intensity maintains good stability (the relative standard deviation is less than 4.4%) during 30 consecutive images, which is extremely important in single-cell ECL imaging.

The quantitative visualization of H_2O_2 at individual Co_3O_4 nanoparticles can further validate the catalytic performance of the Co_3O_4 nanozyme. Thus, we investigated the ECL visualization of different concentrations of H_2O_2 (50 pM–20 μM) at Co_3O_4 nanoparticles in 10 mM PBS containing 200 μM L012. As shown in Fig. 5 and Fig. S3 (ESI†), as the concentration of H_2O_2 increases, the ECL intensity of the light spot gradually increases. The spot intensity of three randomly selected nanoparticles shows a good positive correlation with H_2O_2 concentration. The visualization detection limit is as low as 50 pM, which is much less than the previously reported detection limit (2 μM) under a voltage of 1.0 V.[32] The results demonstrate that the Co_3O_4 nanozyme can effectively catalyze the L012-H_2O_2 system to generate strong luminescence under a low H_2O_2 concentration, endowing this strategy with extraordinary visualization sensitivity and ensuring the possibility of further visualization of single cell membrane proteins.

Imaging analysis of low-abundance proteins on the cell surface is crucial for elucidating the molecular mechanisms and related research on disease progression.[10,33,34] Since the CEA antibody enables the selective recognition of cells that express CEA, MCF-7 cells with overexpressed CEA and HeLa
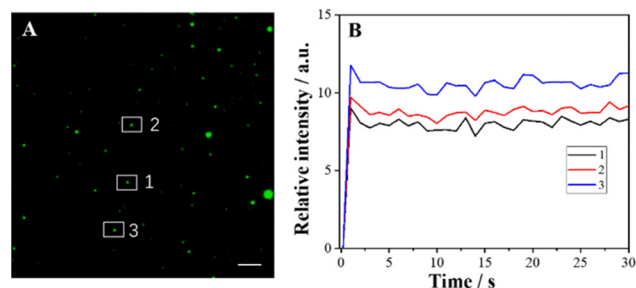

Fig. 4 (A) ECL image of Co_3O_4 at ITO slides; (B) the fluctuation of ECL intensity at three particles labeled as 1, 2 and 3 in (A). The exposure time was 500 ms; the applied potential was 1 V. Scale bar: 5 μm.

Fig. 5 (A) ECL image of Co_3O_4 at ITO slides with different concentrations of H_2O_2; the exposure time was 500 ms, and the applied potential was 1 V. (B) Correlation between the luminescence of three particles and the concentration of H_2O_2. Scale bar: 5 μm.

cells were chosen as the experimental and negative control group, respectively. MTT assay confirms that Co_3O_4 has a low cytotoxicity to MCF-7 cells (Fig. S4, ESI†). The cells were cultured on the ITO slides to the adherent state and fixed with 4% paraformaldehyde to ensure the interaction between the antigen and the antibody.[10] MCF-7 cells show obvious luminescence signals after modifying the functionalized probe Co_3O_4-antibody, while no obvious signal was generated in the HeLa cell region (Fig. 6). These results confirm that the luminescence observed in MCF-7 cells is attributed to the connection of the functionalized probe to the CEA antigen on the cell membrane, so that L012 and H_2O_2 in the solution only produced an enhanced ECL signal on the cell surface. We consider that the Co_3O_4 nanozyme has great potential in imaging other biomarkers on cell membranes owing to its favorable enzyme catalytic activity and biocompatibility.

In summary, we successfully developed a novel Co_3O_4 nanozyme-based ECL imaging approach for the analysis of single cell membrane proteins for the first time. The excellent catalytic performance of Co_3O_4 nanozymes can effectively accelerate the decomposition of H_2O_2 into reactive oxygen species and promote the electrochemical reaction of the L012-H_2O_2 system, inducing an enhanced ECL signal in a very short period. As a result, our ECL imaging system achieves rapid and sensitive imaging of single cell membrane proteins. Furthermore, our proposed Co_3O_4 nanozyme-enhanced ECL
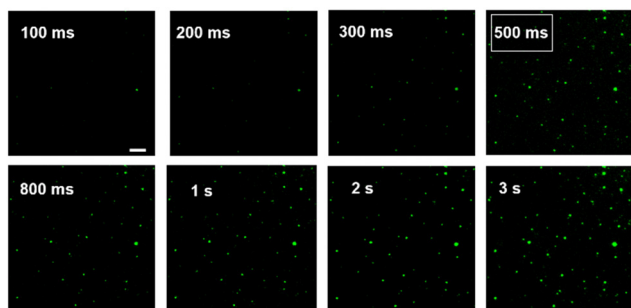

Fig. 3 ECL image of Co_3O_4 at ITO slides with different exposure times; the applied potential was 1 V. Scale bar: 5 μm.

Fig. 6 Bright field (A) and ECL image (B) of MCF-7 cells; bright field (C) and ECL image (D) of HeLa cells on ITO slides. Both MCF-7 and HeLa cells were incubated with Co_3O_4-CEA antibodies and then washed three times. Working solution: 10 mM PBS containing 200 μM L012 and 100 pM H_2O_2. The exposure time was 500 ms, the applied potential was 1 V. Scale bar: 40 μm.

imaging exhibits good versatility, which sheds new light on the ECL imaging of biological molecules.

Conflicts of interest

There are no conflicts to declare.

References

1 W. Miao, *Chem. Rev.*, 2008, **108**, 2506–2553.
2 M. Richter, *Chem. Rev.*, 2004, **104**, 3003–3036.
3 J. Zhang, R. Jin, D. Fang and D. Jiang, *Chem. Res. Chin. Univ.*, 2020, **41**, 2421–2425.
4 M. Zhao, W. Zeng, Y. Chai, R. Yuan and Y. Zhuo, *Anal. Chem.*, 2020, **92**, 11044–11052.
5 Y. Zhang, R. Zhang, X. Yang, H. Qi and C. Zhang, *J. Pharm. Anal.*, 2019, **9**, 9–19.
6 H. Chu, W. Guo, J. Di, Y. Wu and Y. Tu, *Electroanalysis*, 2009, **21**, 1630–1635.
7 N. Wang, Z. Wang, L. Chen, W. Chen, Y. Quan, Y. Cheng and H. Ju, *Chem. Sci.*, 2019, **10**, 6815–6820.
8 Y. Liu, H. Zhang, B. Li, J. Liu, D. Jiang, B. Liu and N. Sojic, *J. Am. Chem. Soc.*, 2021, **143**, 17910–17914.
9 B. Li, X. Huang, Y. Lu, Z. Fan, B. Li, D. Jiang, N. Sojic and B. Liu, *Adv. Sci.*, 2022, **9**, 2204715.
10 J. Zhang, R. Jin, D. Jiang and H.-Y. Chen, *J. Am. Chem. Soc.*, 2019, **141**, 10294–10299.
11 Y. Wang, D. Jiang and H.-Y. Chen, *CCS Chem.*, 2022, **4**, 2221–2227.
12 Y. Lu, X. Huang, S. Wang, B. Li and B. Liu, *ACS Nano*, 2023, **17**, 3809–3817.
13 S. Voci, B. Goudeau, G. Valenti, A. Lesch, M. Jovic', S. Rapino, F. Paolucci, S. Arbault and N. Sojic, *J. Am. Chem. Soc.*, 2018, **140**, 14753–14760.
14 C. Ma, M. Wang, H. Wei, S. Wu, J. Zhang, J. Zhu and Z. Chen, *Chem. Commun.*, 2021, **57**, 2168–2171.
15 G. Valenti, S. Scarabino, B. Goudeau, A. Lesch, M. Jovic', E. Villani, M. Sentic, S. Rapino, S. Arbault, F. Paolucci and N. Sojic, *J. Am. Chem. Soc.*, 2017, **139**, 16830–16837.
16 S. Li, X. Ma, C. Pang, M. Wang, G. Yin, Z. Xu, J. Li and J. Luo, *Biosens. Bioelectron.*, 2021, **176**, 112944.
17 Y. Ma, C. Colin, J. Descamps, S. Arbault and N. Sojic, *Angew. Chem., Int. Ed.*, 2021, **60**, 18742–18749.
18 P. Zhou, L. Ding, Y. Yan, Y. Wang and B. Su, *Chem. Commun.*, 2023, **59**, 2341–2351.
19 W. Guo, P. Zhou, L. Sun, H. Ding and B. Su, *Angew. Chem., Int. Ed.*, 2021, **60**, 2089–2093.
20 H. Ding, W. Guo and B. Su, *Angew. Chem., Int. Ed.*, 2020, **59**, 449–456.
21 H. Ding, P. Zhou, W. Fu, L. Ding, W. Guo and B. Su, *Angew. Chem., Int. Ed.*, 2021, **60**, 11769–11773.
22 J. Wu, X. Wang, Q. Wang, Z. Lou, S. Li, Y. Zhu, L. Qin and H. Wei, *Chem. Soc. Rev.*, 2019, **48**, 1004–1076.
23 S. M. Khoshfetrat, P. Hashemi, A. Afkhami, A. Hajian and H. Bagheri, *Sens. Actuators, B*, 2021, **348**, 130658.
24 L. Jiao, H. Y. Yan, Y. Wu, W. L. Gu, C. Z. Zhu, D. Du and Y. H. Lin, *Angew. Chem., Int. Ed.*, 2020, **59**, 2565–2576.
25 X. Wang, Y. Xu, N. Cheng, X. Wang, K. Huang and Y. Luo, *Catalysts*, 2021, **11**, 638.
26 S. W. Wu, D. Z. Guo, X. C. Xu, J. M. Pan and X. H. Niu, *Sens. Actuators, B*, 2020, **303**, 127225.
27 Y. Chen, X. Gou, C. Ma, D. Jiang and J. Zhu, *Anal. Chem.*, 2021, **93**, 7682–7689.
28 J. Zhang, Z. Huang, Y. Xie and X. Jiang, *Chem. Sci.*, 2022, **13**, 1080–1087.
29 W. Gao, J. He, L. Chen, X. Meng, Y. Ma, L. Cheng, K. Tu, X. Gao, C. Liu, M. Zhang, K. Fan, D. Pang and X. Yan, *Nat. Commun.*, 2023, **14**, 160.
30 J. Dong, L. Song, J. Yin, W. He, Y. Wu, N. Gu and Y. Zhang, *ACS Appl. Mater. Interfaces*, 2014, **6**, 1959–1970.
31 G. Valenti, S. Scarabino, B. Goudeau, A. Lesch, M. Jovic, E. Villani, M. Sentic, S. Rapino, S. Arbault, F. Paolucci and N. Sojic, *J. Am. Chem. Soc.*, 2017, **139**, 16830–16837.
32 J. Zhang, R. Jin, Y. Chen, D. Fang and D. C. Jiang, *Sens. Actuators, B*, 2021, **329**, 129208.
33 T. Gao, B. Wang, L. Shi, X. L. Zhu, Y. Xiang, J.-I. Anzai and G. Li, *Anal. Chem.*, 2017, **89**, 10776–10782.
34 Y. Liu, H. Zhang, B. Li, J. Liu, D. Jiang, B. Liu and N. Sojic, *J. Am. Chem. Soc.*, 2021, **143**, 17910–17914.